

of the General Mills Company of Minneapolis. Launching of the rockoons was supervised by engineers of the General Mills Aeronautical Laboratories. Firing circuits were made at the Naval Research Laboratory through a cooperative arrangement with Herman La Gow and Carl Medrow. The special nose shells were fabricated by Weber Brothers Metal Works of Chicago. The scientific apparatus, including telemeters, was designed

and built at the State University of Iowa. Aerodynamic and mechanical design of the rocket fins and of the nose assemblies was also performed there and the components were built in the shops of the Department of Physics under the able supervision of J. G. Sentinella. Important experimental assistance was given by L. H. Meredith and Lee F. Blodgett of the Cosmic Ray Laboratory.

### Cloud-Chamber Study of Charged $V$ Particles\*

CARL M. YORK, JR., R. B. LEIGHTON, AND E. K. BJØRNERUD  
*California Institute of Technology, Pasadena, California*

(Received March 31, 1954)

An analysis of 103 charged  $V$ -particle decays is presented. These events have been observed with a double cloud chamber operated at 1750-m altitude. The events in the upper chamber appear to have markedly different properties from those in the lower. The particles in the upper chamber have measured properties which are in every respect consistent with those of the  $\kappa$  meson. Their lifetime is in the range  $5 \times 10^{-10}$  to  $2 \times 10^{-8}$  sec; their mass is  $\sim 1000 m_e$ ; their transverse momentum distribution is consistent with a three-body decay scheme; the momentum in the center-of-mass system of their charged decay products is also consistent with three-body decay; and their frequency of production is greater than 0.4 percent of the total number of shower particles observed. On the other hand, the particles observed in the lower chamber have a lifetime in the range  $10^{-11}$  to  $3 \times 10^{-10}$  sec; their transverse momentum distribution is consistent with a two-body decay scheme; their frequency of production is greater than 0.8 percent of the total number of shower particles; they are observed with approximately one-third of the frequency of  $\Lambda^0$  particles; and they apparently can be produced in meson-nucleon collisions. The majority of the particles in the lower chamber are tentatively identified as charged hyperons with the aid of two cases which appear to have proton secondaries. The proposed decay scheme is  $V_1^+ \rightarrow p + \pi^0 + Q$ ; and in order to fit all of the data, the alternate mode of decay,  $V_1^+ \rightarrow \pi^+ + n + Q$  must be introduced. The  $Q$  value is estimated to be  $\lesssim 125$  Mev.

#### I. INTRODUCTION

SINCE the original observation by Rochester and Butler<sup>1</sup> of the decay of a charged particle of mass greater than  $900 m_e$  into a light meson, extensive investigation of the decay of heavy charged particles has been carried out. The evidence has come from three distinct experimental sources, *viz.* cloud chambers in magnetic fields,<sup>2-6</sup> photographic emulsions,<sup>7-10</sup> and multiplate cloud chambers,<sup>11</sup> and has been interpreted in terms of a number of different particles:

(a) The majority of these observations can be explained in terms of a single particle (called a  $\kappa$  meson) of mass about  $1000 m_e$ , which decays into a single, light, charged meson and two or more neutral particles. There is direct evidence that this charged meson is a  $\mu$  meson from its characteristic decay into an electron.<sup>7</sup>

(b) There are also some data suggesting the existence of a different particle, the so-called  $\chi$  meson,<sup>8</sup> of mass about  $1000 m_e$  which decays into a charged  $\pi$  meson and one neutral particle. The evidence relating to the  $\chi$  meson is not very firm at present, but this decay scheme has been considered as a possibility in interpreting the present data.

(c) There is conclusive evidence for the existence of  $\tau$  mesons ( $m \approx 965 m_e$ ) which decay into three  $\pi$  mesons.<sup>9</sup>

(d) Recently, evidence has been presented which indicates that there may be a positively charged  $V$  particle of greater than nucleonic mass which decays into a nucleon and meson.<sup>8-10,12</sup>

(e) Finally, there are rather convincing indications of the existence of a "cascade" decay of a still heavier,

\* Assisted in part by the joint program of the U. S. Office of Naval Research and the U. S. Atomic Energy Commission.

<sup>1</sup> G. D. Rochester and C. C. Butler, *Nature* **160**, 855 (1947).

<sup>2</sup> Seriff, Leighton, Hsiao, Cowan, and Anderson, *Phys. Rev.* **78**, 290 (1950).

<sup>3</sup> R. B. Leighton and S. D. Wanlass, *Phys. Rev.* **86**, 426 (1952).

<sup>4</sup> Armenteros, Barker, Butler, Cachon, and York, *Phil. Mag.* **43**, 597 (1952).

<sup>5</sup> Astbury, Chippindale, Millar, Newth, Page, Rytz, and Sahiar, *Phil. Mag.* **43**, 1283 (1952).

<sup>6</sup> Astbury, Chippindale, Millar, Newth, Page, Rytz, and Sahiar, *Phil. Mag.* **44**, 242 (1953).

<sup>7</sup> C. O'Ceallaigh, *Phil. Mag.* **42**, 1932 (1951).

<sup>8</sup> Report of the Bagnères Conference, 1953 (unpublished).

<sup>9</sup> Lal, Pal, and Peters, *Phys. Rev.* **92**, 438 (1953).

<sup>10</sup> Bonetti, Levi-Setti, Panetti, and Tomasini, *Nuovo cimento* **10**, 1729 (1953).

<sup>11</sup> Bridge, Courant, DeStaebler, and Rossi, *Phys. Rev.* **91**, 1024 (1953). (This reference contains a complete bibliography of the earlier work of this group.)

<sup>12</sup> York, Leighton, and Bjørnerud, *Phys. Rev.* **90**, 167 (1953).

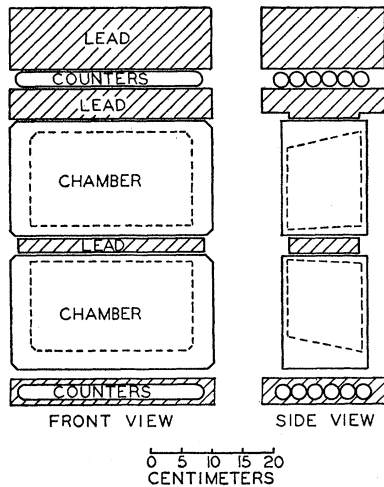


FIG. 1. The arrangement of counters and lead blocks around the cloud chambers. The dotted lines inside the chamber volume indicate the fiducial surfaces used in the lifetime study of Sec. IV. The magnet structure surrounding and supporting the apparatus is not shown.

negatively charged particle which gives rise to a  $V_1^0$  particle and  $\pi$  meson.<sup>4,13</sup>

It is the object of this paper to present additional evidence regarding the nature of  $\kappa$ - and  $\chi$ -meson decay and the existence of the heavy positive  $V$  particle. The cascade decay of heavy negative particles referred to above is not discussed nor is any analysis of  $\tau$ -meson decays included.

## II. APPARATUS AND MEASURING TECHNIQUES

The operation of the cloud chamber used in this experiment has been described in detail by Leighton, Wanlass, and Anderson.<sup>14</sup> However, several improvements and modifications have been made since their work was reported:

(1) A program for the measurement of no-field tracks in order to determine the maximum detectable momentum of the chamber has been carried out. A timing device was installed which turns off the magnet current for fifteen minutes every three hours. Tracks which penetrate the lead block between the two chambers without multiplication or appreciable scattering were selected from the pictures taken during these periods. The curvatures of these tracks were measured in exactly the same way as were the curved tracks obtained with the magnetic field and an histogram of the results was plotted. Two hundred and three tracks were included in the study, and from the width of the resulting distribution of measured no-field curvatures it has been concluded that the maximum detectable momentum for a track 15 cm long in the chamber is 3 Bev/c.

<sup>13</sup> Anderson, Cowan, Leighton, and van Lint, Phys. Rev. **92**, 1089 (1953).

<sup>14</sup> Leighton, Wanlass, and Anderson, Phys. Rev. **89**, 148 (1953).

(2) Several modifications were made in the thermostat system. Provision was made for recording the temperature variation of various parts of the chamber on the same film that was used to photograph the chamber. A study of these variations indicated that there was no observable change in the temperature conditions during the periods in which the magnetic field was turned off. This study also permitted a quantitative check on the gaseous distortions in the chamber. Considerable improvement in the temperature control was progressively attained, but because the events considered in this paper were selected from the total operation period of the apparatus, one can only say that the short-period temperature fluctuations of the cloud chambers were held to about  $\pm 0.1^\circ\text{C}$  during the course of the work.

The momentum and angle measurements were made from the stereoscopic photographs in the same way as were those of Leighton, Wanlass, and Anderson.<sup>14</sup> Ionization estimates were made by three independent observers and a range of possible ionization assigned in the same manner used by the above authors.

Various counter arrangements were used to trigger the apparatus. Of the 71 000 photographs taken of the cloud chamber, 14 000 were taken at 200-m elevation with a coincidence of one or more counters above the chamber and three or more below (this is called a 1-3 selection); 7000 were taken with the same counter selection at 1750 m; 22 000 were taken at 1750 m with 2-3 selection; and 28 000 were taken at 1750 m with 1-3 selection with lead shielding surrounding the lower counters. This shielding was accomplished by means of a cast lead block as shown in Fig. 1 and the counting rate with this arrangement was about  $2.5 \text{ hr}^{-1}$ .

## III. A PRELIMINARY SURVEY OF THE DATA

Some of the especially interesting cases contained in the present data have already been reported.<sup>3,12</sup> The present analysis includes those cases and is based upon a total of 103 photographs of events which could be interpreted as charged  $V$ -particle decays, but not as  $\pi$ - $\mu$  decays or as scattering events. These events

TABLE I. Data on scattering events with observable "recoil blobs." ( $P_1$ =momentum before collision,  $P_2$ =momentum after collision,  $\theta$ =angle of deflection,  $R_{\text{calc}}$ =calculated range of the recoil,  $R_{\text{meas}}$ =projected diameter of the recoil blob,  $p_T$ =transverse momentum of the scattered particle.)

Case	Type	$P_1$ (Mev/c)	$P_2$ (Mev/c)	$\theta$	$R_{\text{calc}}$ (mm)	$R_{\text{meas}}$ (mm)	$p_T$ (Mev/c)
1	$\rho$	—	$420 \pm 70$	$84^\circ$	3.00	$2.1 \pm 0.1$	$415 \pm 70$
2	$\pi^+$	—	$250 \pm 50$	$5^\circ$	0.04	$1.0 \pm 0.2$	$20 \pm 5$
3	$\pi^-$	$30 \pm 7$	$18 \pm 5$	$33^\circ$	0.03	$0.9 \pm 0.2$	$9 \pm 3$
4	$\rho$	$96 \pm 10$	—	$50^\circ$	0.20	$1.0 \pm 0.2$	$73 \pm 8$
5	$\pi^+$	—	$102 \pm 10$	$15^\circ$	0.05	$1.0 \pm 0.2$	$26 \pm 3$
6	$\rho$	—	$720 \pm 130$	$4^\circ$	0.12	$1.0 \pm 0.3$	$50 \pm 10$
7	$\pi^+$	$490 \pm 100$	—	$20^\circ$	1.00	$1.0 \pm 0.2$	$160 \pm 35$
8	$\pi^-$	—	$200 \pm 30$	$24^\circ$	0.30	$1.2 \pm 0.2$	$80 \pm 12$
9	$\pi^-$	$214 \pm 25$	—	$30^\circ$	0.50	$1.5 \pm 0.2$	$108 \pm 15$
10	$\pi^-$	—	$310 \pm 30$	$20^\circ$	0.50	$1.5 \pm 0.2$	$108 \pm 15$

were distinguished from the decay  $\pi$  mesons by the usual criteria derived from the dynamics of the  $\pi$ - $\mu$  decay. The cases which could be interpreted as  $\pi$ - $\mu$  decays are described in the Appendix. In the past<sup>4</sup> it has been considered reasonable to distinguish charged  $V$ -particle decays from scattering events by requiring that at least 75 Mev/ $c$  of transverse momentum  $p_T$  produce no visible recoil track at the point of deflection. However, since no very clear-cut basis for this particular criterion has yet been presented, it was decided to study the matter in some detail.

Ten events exhibiting a blob of ionization at the points of deflection of tracks in the chamber were selected from the last 20 000 pictures studied in this work. Table I summarizes the data for these events giving the nature of the particle (from ionization and momentum), the measured momenta before and after scattering, the angle of deflection, the measured diameter of the projected recoil blob, and the transverse momentum. In each case the recoil was assumed to be an argon nucleus and its range estimated from the curve of Blackett and Lees.<sup>15</sup> These ranges are entered in the column,  $R_{\text{calc}}$ . These data show that the size of the blob is greater in extent than the predicted range of the recoil for all values of  $p_T \lesssim 160$  Mev/ $c$ . This is readily explained by the fact that the tracks observed in the present experiment are pre-expansion tracks, whereas Blackett and Lees used post-expansion tracks in the determination of their curve. During the expansion time of 16 milliseconds for the present chamber the ions diffuse approximately 1 mm. It is clear from these considerations that the critical factor in determining whether or not a recoil nucleus has been produced is not the range of that nucleus, but the *number of ions it forms* in the process of recoiling. In this connection it is worth while to consider the work of Crane and Halpern<sup>16</sup> who have studied the number of droplets formed by the 5-Mev/ $c$  recoil of  $A^{88}$  nuclei *in air*. From their work one can estimate that at least twenty droplets were produced by ions for a recoil momentum of 5 Mev/ $c$ . It is clear that the total number of ions formed must be proportional at least to the energy of the recoil and hence to the square

TABLE II. Classification of charged  $V$ -particle decays according to their sign of charge and place of origin.

Origin	Charge		$N^+/N^-$
	Positive $N^+$	Negative $N^-$	
Above chamber	14	28	$0.50 \pm 0.16$
Plate between chambers	29	14	$2.07 \pm 0.65$
Total	43	42	1.02

<sup>15</sup> Rutherford, Chadwick, and Ellis, *Radiations from Radioactive Substances* (Macmillan Company, New York, 1930), p. 249.

<sup>16</sup> H. R. Crane and J. Halpern, *Phys. Rev.* **56**, 232 (1939). (The authors are indebted to Mr. V. A. J. van Lint for calling their attention to this work.)

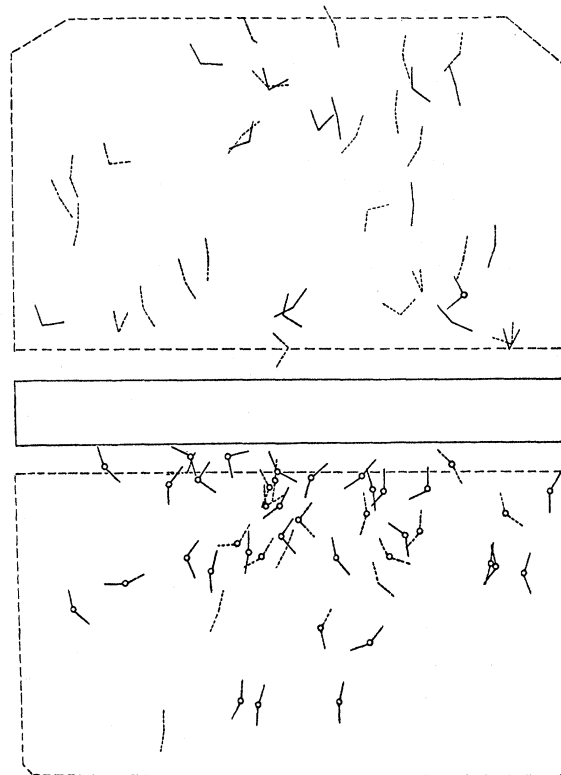


FIG. 2. The distribution of the charged  $V$ -particle decay points. A circle at the apex indicates production in the lead plate separating the two chambers. Solid lines indicate positive particles and dashed lines indicate negatives.

of its momentum. Thus a 50-Mev/ $c$  recoil should produce approximately 2000 ions, which would appear as a very sizeable cluster of droplets. The number of droplets might of course be considerably smaller than the number of ions due to inefficiency of condensation, but an observable blob should certainly remain. It seems clear that the criterion used in this experiment for distinguishing decays from scattering events is sufficiently conservative to account completely for any differences in ion formation between the argon in the present chamber and air, as well as for inefficiency of condensation and statistical fluctuations. This criterion is that if an event for which  $p_T \geq 50$  Mev/ $c$  gives rise to no observable cluster of droplets at the point of deflection, that event is almost surely not a scattering event.

The first treatment of the data consisted of plotting the decay points of the charged  $V$  particles inside the cloud chambers as shown in Fig. 2. In carrying out this scheme two very marked features were noted. First, the decay points were distributed very differently in the two chambers, there being a striking number of very short decay lengths in the lower chamber,<sup>17</sup> and second, the charge ratio of the decaying particles was

<sup>17</sup> This feature was previously noted by Alford and Leighton (see reference 18).

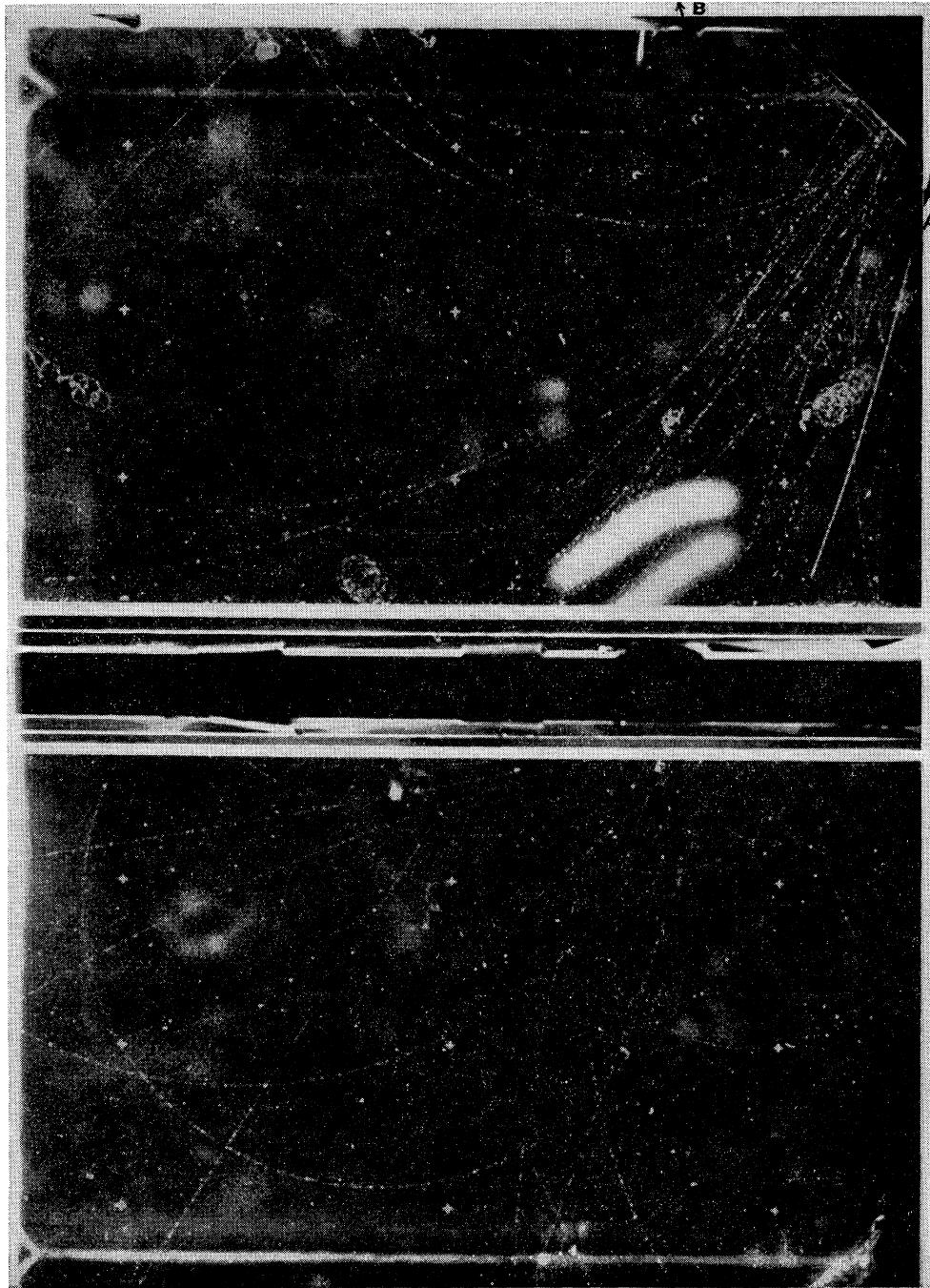


FIG. 3. Event No. 78113, which is listed in Table IV. The heavily ionizing charged  $V$  particle originates in the shower in the upper right-hand corner ( $A$ ) and decays just above the lead plate separating the chambers. The secondary particle is ejected upward and to the left ( $B$ ).

found to be quite different in the two chambers. A convenient way to indicate the asymmetry of charge is set forth in Table II where the number of positively and negatively charged  $V$  particles with origins above the apparatus or in the lead plate separating the two chambers is given. A table of this form has previously been published,<sup>12</sup> and the numbers have simply been brought up to date in the present version. The statistical probability that this (or any greater) charge asymmetry

would be obtained as a fluctuation from a uniform charge distribution in the two chambers is about 0.002.

These marked asymmetries have already been tentatively interpreted in terms of a mixture of long- and short-lived charged  $V$  particles.<sup>12</sup> By considering the relative positions of the production layer and the cloud chamber, those charged  $V$  particles observed in the upper chamber were presumed to be predominantly long-lived particles with a negative excess of about

two to one at their point of production. (This need not imply that a single type of particle is observed, but only that the particles are predominantly long lived.) The charged  $V$  decays in the lower chamber are then supposedly a mixture of both long- and short-lived particles, and from the marked positive excess of this group of decays the short-lived particles should be predominantly if not entirely positively charged.

The next procedure consisted of determining the masses of the particles involved in the charged  $V$  decays from momentum measurements and ionization estimates. A photograph of such a decay event is shown in Fig. 3. A frequency distribution of the mass values has been plotted for all heavily ionizing primaries and secondaries in Fig. 4. It can be concluded that the masses of the measurable primary particles are in agreement with a mass of about  $1000m_e$  and that the secondaries are all light mesons with two outstanding exceptions. These exceptions will be discussed in detail in Sec. VII.

A careful survey of the data was made for possible evidence of the existence of  $\gamma$  rays associated with the decay of the charged  $V$  particles.<sup>11</sup> One might expect to see electron cascades generated in the lead block between the chambers; however, in no case was such a cascade observed. It should be noted that this does not imply that there are no  $\gamma$  rays among the decay products of the charged  $V$  particles, because the thickness of the lead block (about six radiation lengths) makes it a very inefficient detector for low-energy cascade showers.

#### IV. LIFETIMES

The preliminary treatment of the data above suggested that two or more types of charged  $V$  particle with a marked difference in lifetime and sign of charge might exist. The evidence relating to the lifetimes will now be considered in detail.

The necessity for obtaining a sufficiently large, unbiased sample of  $V$ -particle decays of a single type, in order to determine their mean life with any precision, limits the use of cloud-chamber observations unless a definite classification of the particles can be made. The present data do not, in most cases, distinguish between the possible types of charged  $V$  particles. However, *limiting values* of the mean life  $\tau$  of any given set of charged  $V$  decays can be made which do not involve a detailed knowledge of the nature of the particles observed. It is important to stress that the limiting lifetimes thus obtained may refer to an unknown mixture of two or more types of particles, but that even in such a case it may still be possible to obtain meaningful limits upon the lifetimes of the constituents of such a mixture.

The method used in the reduction of the data was essentially the same as that used by Alford and

Leighton.<sup>18</sup> The minimum requirements of determination of the sign of charge and the existence of an approximate origin were satisfied for 84 charged  $V$  events at the time the analysis was carried out. Of these, 62 cases had their point of decay inside the fiducial surfaces. The rather large fraction, 26 percent, excluded by the fiducial limits can be compared to the 14 percent of the neutral  $V$  particles similarly excluded by Alford and Leighton. Most of the excluded charged  $V$  events are near the front glass or back piston of the chamber where neutral  $V$ 's are difficult to identify.

The experimental quantities which were used in this analysis are as follows:  $x_i$  is the distance (in cm) between the point of entrance of the  $i$ th particle into the region of the chamber inside the fiducial limits and the point of decay.  $D_i$  is the corresponding distance (in cm) between the point of entrance and the point at which the particle would have left the fiducial region had it not decayed.  $D_i$  is usually called the gate length.  $t_i$  and  $T_i$  are the times taken to traverse the distances  $x_i$  and  $D_i$ , respectively, in the rest-system of the  $V$  particle. These proper times are related to the measured distances by the equation

$$t_i = (x_i/c)(M/P_i c) = (x_i/c)(1/\beta_i \gamma_i), \quad (1)$$

where  $M$  is the mass of the particle in Mev and  $P_i$  is the measured momentum in Mev/c. A similar relation can be written for  $T_i$ . The quantities  $c$ ,  $\beta$ , and  $\gamma$  have the usual significance.

In each case it is necessary to have an estimate of  $\beta_i \gamma_i$ , and if the particle has a known mass and measurable momentum, this product is easily obtained. However, since one rarely knows these two quantities, an alternate procedure must be employed. Upper and lower limits can be assigned to  $\beta_i \gamma_i$  in each case and these quantities can, with the aid of Eq. (1), be used

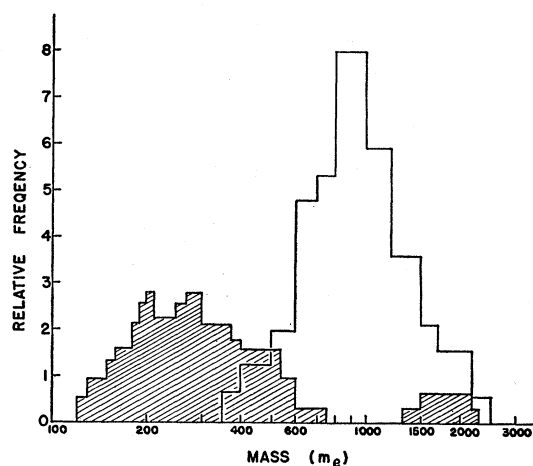


FIG. 4. Frequency distribution of the measured masses. The unshaded area gives the masses of the primary particles and the shaded area the masses of the secondaries. Ten positive and seven negative primaries are represented.

<sup>18</sup> W. L. Alford and R. B. Leighton, Phys. Rev. **90**, 622 (1953).

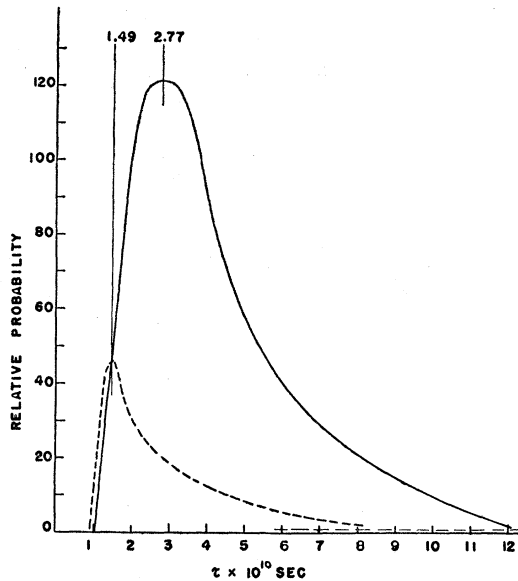


FIG. 5. Plots of the likelihood function for the two limiting lifetime estimates obtained from the data of the lower chamber. The solid curve is for the estimate of the upper limit and the dashed curve for the lower limit of the mean life.

to determine lower and upper limits, respectively, for the values of  $t_i$  and  $T_i$ .

In all but four of the 62 cases it was possible to assign an upper limit to the ionization of the primary particle. In 39 of the remaining cases the ionization was indistinguishable from minimum, and in these cases the upper limit was taken to be one and one half times minimum. These upper limits determined lower limits to  $\beta_i \gamma_i$  in each case and, by Eq. (1), upper limits to  $t_i$  and  $T_i$ .

On the other hand, the sign of charge, as determined from the direction of curvature of the *parent* particle was in all cases the same as that obtained from that of the *secondary* particle, which had easily measured momenta. Thus the momenta of the primary particles themselves were presumably within the upper limit set by the chamber distortions, so that this limit, 3 Bev/c, could be used as an *upper limit to the momentum of each primary particle*. Taking the mass of the primary particles as  $1000m_e$  or greater, the upper momentum limit thus obtained gives a lower limit to  $t_i$  and  $T_i$ .

Although this latter method is useful, its limitations ought to be emphasized. If the sample of decay events being treated is predominantly of one sign of charge (as is the case in the present application) and if the chamber has a small, *systematic* gas distortion of a type which appears as a smooth curve, then the estimates of the sign of charge of the primary particle might easily be biased to give better agreement with the true sign of charge than would have been obtained in the absence of the distortion. If such were the case, the maximum detectable momentum might no longer be a conservative estimate of the upper limit to the

momentum of the  $V$  particle. It is clear that such a bias will be more important for short tracks near the edges of a chamber than for long tracks near the center. Thus the interpretation of any results obtained with this method must be made with due caution.

In order to treat the whole sample uniformly, only the two methods just described were used to establish limits to  $t_i$  and  $T_i$ , including 14 cases for which the momentum of the primary particle was measurable. This procedure has advantages in that it does not bias the sample by the selection of slow particles with long tracks for which the momentum is readily measurable, and it permits most of the observed cases to be included in the analysis. The data on the 58 cases finally included in the lifetime analysis thus consist of two sets of values of  $t_i$  and  $T_i$ , corresponding to an upper and a lower limit to each. Of the 30 cases in the lower chamber, four negative particles apparently had their origin in the lead above the upper chamber, but were treated in this analysis as if they originated in the plate between the chambers. In Table III the number of cases observed in each chamber, the average limiting values of  $t$  and  $T$ , the average value of  $x/D$ , and the ratio of the number of positive to the number of negative particles in each chamber are given. These data show the marked difference between the two chambers and the necessity for treating each chamber separately. It is seen that the limiting values of  $\bar{T}$  for the two chambers are very nearly the same. This would be expected for identical chambers, provided no bias due to the selection of groups of particles with greatly different average velocities has been introduced.

(a) *Upper chamber*: For gate times which are small compared to the mean lifetime of the decaying particles, one expects the decay points to be uniformly distributed throughout the chamber, and hence the average value of  $x/D$  to be equal to one-half. It is immediately apparent from Table III that such is the case in the upper chamber, so that the "apparent" lifetime of the particles in the upper chamber is probably much greater than the average gate time, i.e.,

$$\tau(\text{upper chamber}) > 4.5 \times 10^{-10} \text{ sec.}$$

TABLE III. Comparison of the events used in the lifetime study. ( $r$  is the ratio of positive to negative particles,  $\langle x/D \rangle_{Av}$  is the average value of the ratio of decay length to gate length,  $\bar{t}$  is the average time of flight in the chamber before decay, and  $\bar{T}$  is the average gate time.)

	No. of cases	$r = \frac{N_+}{N_-}$ <sup>a</sup>	$\langle x/D \rangle_{Av}$ <sup>b</sup>	$\bar{t}$ (10 <sup>-10</sup> sec)		$\bar{T}$ (10 <sup>-10</sup> sec)	
				Upper limit	Lower limit	Upper limit	Lower limit
Upper chamber	28	0.65 ± 0.25	0.46 ± 0.10	3.2	1.5	6.1	2.9
Lower chamber	30	2.00 ± 0.77	0.31 ± 0.09	1.7	0.8	5.4	2.4

<sup>a</sup> The errors quoted for  $r$  are probable errors.

<sup>b</sup> The errors quoted for  $\langle x/D \rangle_{Av}$  are 95 percent confidence limits, *not* the usual probable errors.

That these events do not necessarily consist of a single type of particle is indicated by the fact that one negative case in this chamber could be identified as a cascade decay such as those recently reported.<sup>13</sup> A careful search was made for additional cases where a neutral  $V$  particle might have decayed in the plate, but none was found.

(b) *Lower chamber*: For the sample of 30 cases in the lower chamber the average ratio ( $x/D$ ) is significantly different from 0.50, as can be shown by conventional statistical methods. A maximum-likelihood analysis<sup>18</sup> was therefore made to determine *limiting values* of  $\tau$ . The likelihood function

$$L = \prod_{i=1}^N \frac{1}{\tau} \frac{\exp(-t_i/\tau)}{1 - \exp(-T_i/\tau)}, \quad (2)$$

which is proportional to the probability of having obtained the particular set of experimental data, can be shown to have the property that if  $t_i$  and  $T_i$  are consistently overestimated, each by the same factors  $\alpha_i$ , the best value of  $\tau$  determined from this likelihood function is then correspondingly an overestimate of the lifetime of the sample, and similarly for underestimates.

The best value of the mean life (that value of  $\tau$  for which  $L$  is a maximum) is given by

$$\tau = \frac{1}{N} \sum_{i=1}^N \left( t_i + \frac{T_i}{\exp(T_i/\tau) - 1} \right). \quad (3)$$

By expanding the exponential functions in the parentheses, this can be written in a form more convenient for the calculation of  $\tau$ :

$$\tau \approx \frac{\sum T_i^2 - (1/60)\tau^{-2} \sum T_i^4}{6\sum T_i - 12\sum t_i}. \quad (4)$$

The calculation of  $\tau$  for the two limiting sets of data gives

$$\begin{aligned} \tau(\text{upper limit}) &= 2.77 \times 10^{-10} \text{ sec}, \\ \tau(\text{lower limit}) &= 1.49 \times 10^{-10} \text{ sec}. \end{aligned}$$

The calculation of the likelihood function  $L$  was performed to determine the significance of these values, and the results are shown in Fig. 5. The ordinates of the curves were normalized to the value of  $L$  for  $\tau \rightarrow \infty$ , i.e.,

$$L = \prod_{i=1}^N \frac{1}{T_i}, \quad \text{as } \tau \rightarrow \infty.$$

In order to estimate the probable errors for these limiting values of the mean lifetime, the probability that  $\tau \leq \tau_0$  must be calculated. This probability,  $F(\tau_0)$  is given by the integral

$$F(\tau_0) = \int_0^{\tau_0} L(\tau) d\tau.$$

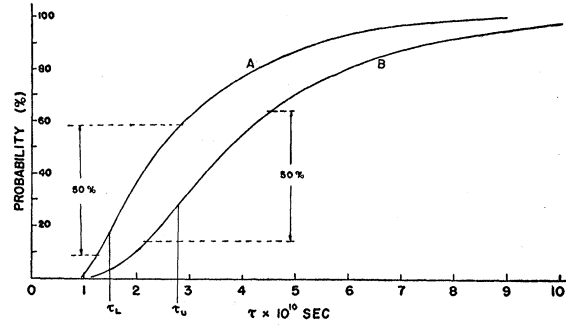


FIG. 6. The plot of  $F(\tau_0) = \int_0^{\tau_0} L(\tau) d\tau$  versus  $\tau$ , together with the assigned 50 percent confidence limits to each of the limiting estimates of the lifetime found in the lower chamber.

The integration can be performed graphically and the resulting curves are given in Fig. 6. As indicated in the figure, 50 percent confidence limits have been used to determine the probable errors on the two limiting values of the mean lifetime. The result is

$$\left[ 1.5 \begin{pmatrix} +1.3 \\ -0.3 \end{pmatrix} < \tau < 2.8 \begin{pmatrix} +2.0 \\ -0.6 \end{pmatrix} \right] \times 10^{-10} \text{ sec}.$$

These limits can be associated with the mean life of a specific particle only if the sample is composed entirely of particles of that type. If the sample is pure, then these limits indicate that the particle has a lifetime between them. If the sample is a mixture of particles, then the upper limit indicates that at least one type of particle with lifetime less than  $2.8 \times 10^{-10}$  sec is contained in the sample and the lower limit implies that another type of particle with lifetime greater than  $1.5 \times 10^{-10}$  sec is present. However, in view of the earlier remarks about possible bias in the determination of this lower limit, no very great significance will be attached to it.

## V. ADDITIONAL PROPERTIES OF THE DECAY OF CHARGED $V$ PARTICLES

In addition to the lifetimes discussed in the previous section several other measured properties of charged  $V$  particles deserve some detailed consideration. These are: the nature of the particles involved in the decay, the distribution of the transverse momenta of the secondary particles, and the value of the momentum  $p^*$  of the secondary particle in the center-of-mass system of the decay. Because the lifetime study showed a marked difference in the charged  $V$ 's decaying in the upper and lower chambers, it seems reasonable to investigate the remaining decay properties by analyzing the events in the two chambers separately to bring out any further differences.

(a) The nature of the primary particles can be inferred in part from the direct measurement of their masses (see Fig. 4 above). However, it should be noted that the requirements of measurability demand that the particles travel a considerable distance at

low velocity before decaying, so that any sample of such mass measurements will be strongly biased in favor of particles with long mean lives. *It is interesting that of the seventeen heavily ionizing, measurable primaries contained in the data all except four are observed in the upper chamber and contribute to the long mean lifetime observed there.* As mentioned above, four negative particles were observed to traverse the lead plate between the chambers before decaying, but these give no information regarding the nuclear interaction of the particles because it would not have been possible to identify a star in the plate produced by a charged  $V$  particle.

In Fig. 4 it is seen that the masses of all except two of the secondary particles are consistent with either that of a  $\pi$  or  $\mu$  meson. The two exceptions will be treated in detail in Sec. VII below. No secondary particle was observed to decay in flight, and only four traversed the lead plate separating the chambers. None of the secondary particles produced a nuclear interaction and therefore no conclusion can be drawn with regard to whether these were  $\pi$  or  $\mu$  mesons.

(b) In considering the transverse momentum distribution of the secondary particles emitted in charged

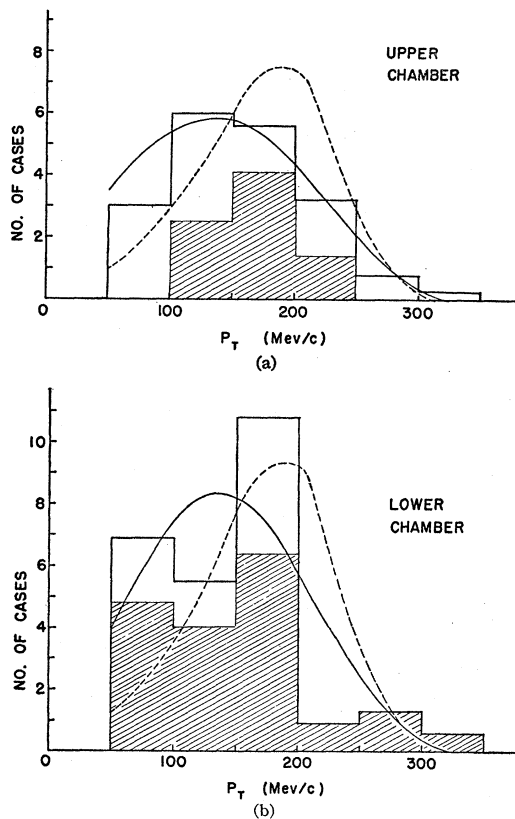


FIG. 7. Frequency distributions of the measured transverse momenta for the upper and lower chambers. The shaded areas indicate the contribution of positive particles to the total distribution. The solid curve is calculated for a three-body decay ( $p^*=240$  Mev/c) and the dashed curve for a two-body decay ( $p^*=216$  Mev/c).

$V$ -particle decay, the data from the upper and lower chambers have been treated separately. The resulting distributions are given in Figs. 7(a) and 7(b). Here the number of cases per 50-Mev/c interval is plotted against the transverse momentum. The shaded areas indicate the contribution of positive particles to the total distributions. In accord with the minimum-transverse-momentum criterion required to eliminate  $\pi$ - $\mu$  decays and scattering events, these distributions do not have any cases with  $p_T$  less than 50 Mev/c. The smooth curves represent the calculated distributions for two- and three-body decay with fifteen percent experimental errors folded in. The three-body decay curve has been calculated by assuming that a  $1000m_e$  primary particle ( $\kappa$  meson) decays into a  $\mu$  meson and two zero-rest-mass particles.<sup>19</sup> The two-body curve has been calculated for a momentum of the charged meson of 216 Mev/c in the center-of-mass system of the decay. This value of the momentum is that assumed for  $\chi$ -meson decay and has been plotted for ease of comparison. The areas under the curves for  $p_T > 50$  Mev/c have been normalized to be equal to the total areas contained in the frequency distributions of the experimental data.

By cutting off the distributions at 50 Mev/c, bias of the data is reduced due to contamination from scattering events as well as due to the difficulty of observing low transverse momentum cases. It is clear that such cases will in general involve small angles of deflection which might easily be overlooked in searching through the film for charged  $V$  events. Because the transverse momentum depends upon the measurability of the momentum of the secondary particle, the distributions of transverse momentum will be slightly biased to include more of the short-lived primary particles than of the longer-lived ones. However, a relatively inconsequential bias will result and the small amount of data does not warrant a correction for this effect.

Because there are relatively few cases involved in these distributions, it is not possible to make significant statistical tests of the "goodness of fit" of the theoretical curves and the experimental data. It is clear that many more cases would be needed to distinguish clearly between two- and three-body decay schemes. On the other hand, although the level of statistical significance is low, the transverse momentum distributions in the two chambers would appear to indicate some differences in the type of decay involved.

(c) In treating the determination of the momentum  $p^*$  of the secondary particle in the center-of-mass system, care has been taken not to introduce any bias into the data. All cases in which the primary particle was judged to be heavily ionizing and the transverse momentum of the secondary was measurable are listed in Table IV. The limits of ionization of the primary particle are used to obtain the limits on the

<sup>19</sup> C. M. York, Phil. Mag. 43, 985 (1952).



TABLE IV. Data on 9 cases with both momenta measurable and 5 cases with primary ionization  $>1.5\times$  minimum and secondary momentum measurable.  $A$  signifies an origin above the chamber and  $P$  and origin in the plate.

Case	Origin and sign	$p_1$ (Mev/c)	$p_2$ (Mev/c)	$(I/I_0)_1$	$(I/I_0)_2$	$\theta$	$p_T$ (Mev/c)	$p^*$ (Mev/c)	$x$ (cm)	$D$ (cm)
7029	$A(-)$	$185\pm 20$	$150\pm 10$	6-10	1.3-2.0	$85^\circ$	$150\pm 10$	160-155	11.5	13.2
17620	$A(-)$	$1050\pm 300$	$750\pm 70$	$<1.5$	$<1.5$	$8^\circ$	$109\pm 10$	$179\pm 20^a$	3.8	15.5
25343	$P(+)$	$185\pm 30$	$215\pm 30$	1.5-2.5	$<1.5$	$51^\circ$	$165\pm 20$	181-165	4.3	8.8
26622	$P(-)$	—	$295\pm 10$	1.5-2.5	$<1.5$	$33^\circ$	$160\pm 5$	160-180	5.4	14.7
31589	$P(-)$	—	$265\pm 20$	1.5-3.0	$<1.5$	$40^\circ$	$170\pm 20$	171-182	2.3	14.4
32530	$A(-)$	$465\pm 70$	$590\pm 70$	$<1.5$	$<1.5$	$29^\circ$	$285\pm 40$	$320\pm 80^a$	6.4	14.7
36726	$A(+)$	—	$140\pm 20$	1.5-3.0	$<1.5$	$108^\circ$	$135\pm 20$	304-210	4.5	15.7
40840	$P(+)$	$95\pm 20$	$184\pm 20$	6-12	$<1.5$	$87.5^\circ$	$184\pm 20$	197-190	4.1	7.9
52999	$A(+)$	$165\pm 30$	$215\pm 20$	15-30	1.3-2.0	$121^\circ$	$185\pm 20$	250-234	2.5	6.2
54056	$P(-)$	—	$325\pm 75$	1.5-3.0	$<1.5$	$13^\circ$	$73\pm 15$	112-177	0.8	13.7
55482	$P(-)$	—	$182\pm 20$	1.5-2.5	2-4	$53.5^\circ$	$146\pm 15$	193-152	—	—
60452	$A(+)$	$255\pm 40$	$212\pm 7$	6-12	$<1.5$	$99^\circ$	$210\pm 7$	245-230	—	—
65550	$A(-)$	$1500\pm 600$	$120\pm 30$	$<1.5$	$<1.5$	$41.5^\circ$	$79\pm 20$	$213\pm 50^a$	11.9	13.9
78113	$A(+)$	$107\pm 4$	$251\pm 8$	10-15	$<1.5$	$133^\circ$	$182\pm 6$	310-296	—	—

<sup>a</sup>  $p^*$  calculated assuming a mass of  $1000m_e$  for the primary particle.

velocity of the center-of-mass system of the decay. By applying a Lorentz transformation to the longitudinal component of momentum of the secondary particle, the corresponding limits to  $p^*$  are obtained. For completeness several cases in which the primary particle was essentially at minimum ionization but had a measurable momentum are included. These cases are indicated in the table and  $p^*$  has been calculated for them by assuming that the primary particle has a mass of  $1000m_e$ . As mentioned earlier, the table includes the values of the decay length  $x$  and the potential path length  $D$  for all of the cases.

The small number of cases and the errors inherent in the observations preclude any detailed interpretation of the values of  $p^*$ ; however, the spread of values, especially in the upper chamber, seems to favor a non-unique value of  $p^*$ . This could result from either a mixture of several types of two-body decay, or from a single three-body decay scheme. In particular, the distribution is completely consistent with what might be expected for  $\kappa$ -meson decay.

## VI. THE PRODUCTION OF CHARGED $V$ PARTICLES

The most direct information with regard to the production of the charged  $V$  particles can be obtained from those events proceeding from an interaction in the lead plate separating the two cloud chambers. In Table V, 43 such cases have been classified according to the nature of the particle which initiated the nuclear event. It is seen that most of the events were caused by particles which were themselves secondaries of penetrating showers. A similar classification of data taken with the same apparatus and over the same period of time has been made for 118 *neutral*  $V$  particles and these results are included in the table. There is a striking similarity between the two sets of numbers. It seems reasonable to suggest that the charged  $V$  particles observed in the lower chamber are produced by a mechanism which is very similar to that of neutral  $V$  particles and that meson-nucleon collisions in lead can give rise to charged  $V$  particles. (A similar result

has been obtained at the Brookhaven Laboratory<sup>20</sup> where artificially produced  $\pi$  mesons have bombarded hydrogen to produce charged  $V$  particles.) In each category the ratio of charged to neutral  $V$  particles has been taken and is seen to be the same for each within the limits of the statistics. This indicates that charged  $V$  particles in the lower chamber are observed with about one-third the frequency of neutral  $V$  particles independently of the character of the producing particle.

The frequency of production of charged  $V$  particles relative to the total number of shower particles has been calculated separately for the two chambers, using a method similar to that of Barker *et al.*<sup>21</sup> The geometry used in this experiment is shown in Fig. 1. In the lower chamber, only production in the lead block separating the two chambers has been considered. In calculating the curves shown in Fig. 7 it has been assumed (a) that particles of unique mass are observed to decay in each chamber, (b) that all of the shower particles have a differential momentum distribution of the form  $P^{-3}dP$  for momenta in excess of 1 BeV/c, (c) that the penetrating showers are produced uniformly throughout the production layer, (d) that the cross section for penetrating shower production is insensitive

TABLE V. The number of penetrating showers occurring in the lead plate between the chambers giving rise to  $V^\pm$  particles, classified according to the type of primary. Similar data for neutral  $V$  particles is included and the ratio  $R$ , calculated for each category.

Type of event	$V^\pm$	$V^0$	$R(V^\pm/V^0)$
Charged primary, accompanied by other shower particles	27	83	$0.32\pm 0.07$
Charged primary, unaccompanied	11	21	$0.52\pm 0.19$
Neutral primary, (acc. and unacc.)	5	14	$0.36\pm 0.18$
Totals	43	118	$0.36\pm 0.05$

<sup>20</sup> Fowler, Shutt, Thorndike, and Whittemore, Phys. Rev. **93**, 861 (1954).

<sup>21</sup> Barker, Butler, Sowerby, and York, Phil. Mag. **43**, 1201 (1952).

to the energy of the primary particles. For simplicity it is also assumed, (e), that all of the shower particles and decaying charged  $V$  particles travel vertically downward. If the detection efficiency as a function of the lifetime of the decaying particles is evaluated using the above assumptions, the frequency of production as a function of lifetime can then be obtained from the observed ratio of decaying  $V$  particles to total number of shower particles. From 1045 counted shower particles with momenta above 1 Bev/ $c$ , a weighted<sup>22</sup> total of 35 600 particles produced in the lead block above the upper chamber and 8400 produced in the lead between the chambers were estimated to have been seen during the course of the experiment. These are to be compared to 41 charged  $V$ 's with momenta greater than 1 Bev/ $c$  observed in the upper chamber and 43 in the lower. The resulting curves of the frequency of production as a function of the mean lifetime are plotted in Fig. 8. For both curves a mass of  $1000m_e$  for the decaying particles has been assumed, but the dotted line  $A'$  lying just above the curve for the lower chamber has been calculated assuming a mass of  $2000m_e$  to show the small effect of this assumption. The vertical lines in the figure indicate the limits on the mean lifetimes estimated in Sec. IV and the attached arrows indicate the range in which the true mean lifetimes for the two groups of particles probably lie.

The particles in the lower chamber have a frequency of production which is insensitive to the lifetime for a fairly large range of values of the lifetime. An estimate of the lower limit to the lifetime of these particles can be obtained by assuming that their frequency at production is ten percent of all of the shower particles. This gives a lower limit of about  $10^{-11}$  sec. If this same criterion of ten percent is applied to the upper chamber,

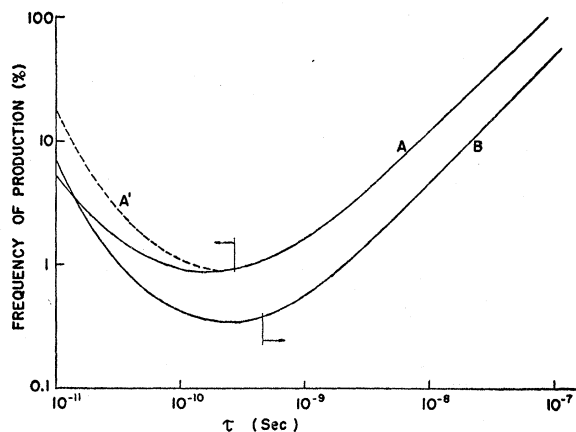


FIG. 8. The frequency of production vs lifetime curves for the upper chamber (curve B) and the lower chamber (curve A). The dashed curve,  $A'$ , is calculated for the lower chamber assuming a mass of  $2000m_e$ . The lines with arrows attached to the curves, indicate the limiting lifetimes obtained in Sec. IV.

<sup>22</sup> It was necessary to weight the total according to the number of pictures taken with each counter arrangement.

one can estimate an upper limit to the lifetime of the particles decaying there of about  $2 \times 10^{-8}$  sec.

## VII. THE $V_1^+$ PARTICLE

In the previous sections several marked differences in the decay properties of the charged  $V$  particles in the upper and lower chambers have been noted. One of these differences which was briefly mentioned in the discussion of the masses of the secondary particles in Sec. V above, is that two charged  $V$  particles having secondary particles with masses greater than  $1300m_e$  were found in the lower chamber. Both are positive and both have origins in the lead plate separating the two chambers. It should be emphasized that while these heavy secondaries are quite consistent in mass and charge with protons, the mass measurements do not exclude the possibility that they are somewhat lighter or heavier than protons. A tentative interpretation of these events as being examples of the decay of a charged counterpart of the familiar  $V_1^0$  particle has already been made.<sup>12</sup> Table VI contains the data relevant to these two cases. In the preliminary discussion of these events the question of possible alternative interpretations was not treated for the sake of brevity. However, at least two other possible interpretations require some detailed consideration. The first is the possibility that these  $V_1^+$  events are in fact  $V_1^0(\Lambda^0)$  events in which the  $\pi$ -meson decay product is ejected backwards along the line of flight of the  $V_1^0$  particle. The second is that a proton arising in a nuclear interaction in the lead might scatter in the argon gas of the chamber to produce the observed event.

Let us first consider the probability that the  $\pi$  meson of a  $V_1^0$  decay would be ejected backwards along the line of flight of the parent  $V_1^0$  particle. A careful, unprejudiced reprojection of the events was made to determine the accuracy with which the primary track could be lined up with the origin of the nuclear event in the lead block. In the first case this was  $\pm 2$  mm at a distance from the decay point of 4.2 cm and in the secondary the uncertainty of alignment was  $\pm 2.5$  mm at 2.9 cm. If random emission of the  $\pi$  meson in the laboratory system is assumed, one can calculate that the probability of occurrence for the first case is  $1/1600$  and  $1/700$  for the second. The *a priori* chance of observing two such independent events is thus very small indeed. It should be noted that the effect of considering the motion of the center-of-mass system is to decrease these probabilities. Furthermore, in these considerations we have ignored the requirement that the momenta of the  $\pi^-$  and  $p^+$ , transverse to the direction of flight of the  $V_1^0$  particle, must balance. This requirement would not be fulfilled for either of these cases if the  $V_1^0$  particle were produced in the nearby nuclear interaction. Thus it would be necessary either to postulate a multi-body decay for these particles or alternatively that they were produced elsewhere. Either of these possibilities would introduce

TABLE VI. Summary of the data pertaining to two cases of  $V_1^+$  decay.

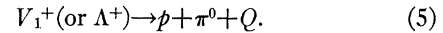
Case	$P_{pri}(\text{Mev}/c)$	$I_{pri}(\times\text{min})$	$M_{pri}(m_e)$	$P_{sec}(\text{Mev}/c)$	$I_{sec}(\times\text{min})$	$M_{sec}(m_e)$	$\theta$	$P_T(\text{Mev}/c)$
1	—	3-7	—	$360\pm 60$	3-7	1300-2300	$20^\circ$	$125\pm 25$
2	—	2-4	—	$520\pm 75$	2-4	1300-2200	$18^\circ$	$160\pm 40$

an additional improbability into the interpretation of these events as  $V_1^0$  decay.

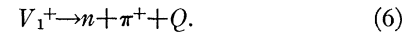
In considering the possibility that the  $V_1^+$  events are scattered protons, one ought first to inquire as to the probability of such an event. A careful survey of the total number of protons produced in nuclear interactions in the plate was carried out to determine the total path length of such proton tracks in the argon gas of the chamber. The criteria for selecting the tracks were that they originate in an interaction in the plate and that they have momenta and ionizations compatible with that of a proton. The protons were chosen from pictures taken with the various counter arrangements used, and from a total of 31.3 m of measured track, a weighted total of 570 m was estimated to have been observed throughout the course of the experiment. It is clear from the discussion of elastically scattered particles given in Sec. III above, that a recoil nucleus should be readily observable at these transverse momenta. However, it is possible that an inelastic scatter of the proton occurs with perhaps the ejection of one or more neutrons to balance the momentum. In estimating the cross section for such a process it is clear that not all angles of scattering will contribute to the type of event that is being considered here. For a given incident momentum and angle of deflection, transverse momentum balance requires a recoiling particle in the nucleus with a momentum at least equal to the transverse momentum of the deflected particle. When this momentum is sufficiently high, charged-particle emission will become probable and the event would not be considered a case of scattering. The momenta of the incident particles in the two events under discussion are unknown, but for the sake of discussion, assume that in both cases the incident particle has 350-Mev/ $c$  momentum, the lower of the two observed values of the momentum of the scattered particle. This is an extremely conservative value, especially if the cases represent inelastic scatters. If the transverse momentum at which charged particle emission becomes likely is taken to be 200 Mev/ $c$ , the maximum angle of deflection that needs to be considered is  $35^\circ$ . This value of the transverse momentum has been chosen so that a single nucleon inside the nucleus would be given a kinetic energy of 21 Mev. Since the change in the longitudinal component of momentum has been ignored, this value of the transverse momentum is considered to be conservative. In view of the elastic scattering criterion established above, no case of  $p_T < 50$  Mev/ $c$  would have been considered. Such a  $p_T$  corresponds in these events to an angle of deflection of  $8^\circ$ , so that the angular interval

to be considered has been chosen to lie between  $8^\circ$  and  $35^\circ$ . The differential inelastic scattering cross section is assumed to be geometric and uniform for all angles of emission in the range of angles considered. Under the foregoing assumptions the mean free path for observing the above type of events in the argon gas of the cloud chamber is 6300 m and the probability of observing two events in the examined track length is then 0.0074. In view of the way in which the values were chosen in calculating this number, it may be considered an upper limit to the probability of observing the two events under discussion. Hence this alternative explanation of the  $V_1^+$  events is not considered satisfactory.

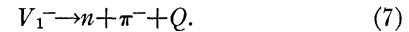
As a result of these considerations the suggestion has been made<sup>12</sup> that the short-lived particles observed in the lower chamber are hyperons which decay according to the scheme,



Because a large number of the short-lived particles give rise to secondary particles whose masses are consistent with that of light mesons, it is inferred that the charge-exchange counterpart of the above reaction is also observed, *viz.*,



Although there is no direct evidence in the present data, it is possible that some of the short-lived negative particles observed in the lower chamber represent the decay scheme,



### VIII. CONCLUSIONS

From the analysis of the data obtained in the two cloud chambers, it seems quite likely that the charged  $V$  particles observed in this experiment are composed of at least two types with quite different properties. The events in the upper chamber are predominantly due to a particle of mass about  $1000m_e$  which decays into a light meson with a mean lifetime considerably greater than  $5 \times 10^{-10}$  sec and less than  $2 \times 10^{-8}$  sec. A study of the transverse momentum and momentum in the center-of-mass system of the secondary particle indicates that there is probably more than one additional neutral particle involved in the decay. From a consideration of the maximum value of the transverse momentum and the rest mass of the primary particle it seems likely that these neutral particles are of very small rest mass and presumably are neutrinos and/or photons. The frequency of production of these particles is greater than 0.4 percent of the total number of

shower particles. The properties of these  $V$  particles are in every respect consistent with those of the  $\kappa$  meson,<sup>7</sup> and similar in every way to the properties deduced from earlier cloud chamber work employing a similar geometric arrangement of the apparatus.<sup>4,21</sup>

The events in the lower chamber have a mean lifetime of less than  $3 \times 10^{-10}$  sec and greater than  $10^{-11}$  sec. Although several of the events in this chamber are probably  $\kappa$  mesons, as indicated by mass measurements on the primaries, some other much shorter-lived particle must predominate to give such a low upper limit to the mean life of the sample. This particle apparently decays most of the time into a light meson and is predominantly positive. The transverse momentum distribution indicates that probably a two-body decay occurs with a momentum in the center-of-mass system of about 200 Mev/ $c$  or less for the secondary particles. The frequency of production of these events is equal to or greater than about 0.8 percent of the total number of shower particles. The two  $V_1^+$  events discussed in detail in Sec. VII above have led to the suggestion that these short-lived particles in the lower chamber are hyperons with at least the two alternate modes of decay given by (5) and (6) above. However, if one accepts neither the interpretation of the  $V_1^+$  cases nor the assumption that the charge exchange counterpart of the decay can occur, the evidence presented above still requires the introduction of a short-lived particle with a rather high rate of production. The observed frequency of occurrence, and the apparent long lifetime, of the much discussed  $\chi$  meson<sup>8</sup> does *not* appear to satisfy the requirements imposed by the present data. However, the small number of observed cases of  $\chi$  mesons, as well as of charged  $V$  particles in this experiment, make it impossible to exclude completely the possibility that the particles observed in the lower chamber are  $\chi$  mesons.

On the other hand, with the acceptance of a charged hyperon as the short-lived particle in the lower chamber, several inferences can be drawn from the data. From the upper limit of the transverse momentum of about 200 Mev/ $c$ , the  $Q$  value of the decay scheme (6) can be estimated to be approximately 125 Mev, or less, in agreement with the values reported at the Bagnères Conference<sup>8</sup> for the hyperons observed in photographic emulsions. The striking similarity of production of these charged hyperons with the neutral hyperons ( $V_1^0$  particles) as shown in Table VI indicates that they are produced by similar mechanisms. The fact that they are observed with one-third the frequency

of the neutral  $V$  particles can in part be attributed to their shorter lifetime and perhaps to a higher energy threshold for production. The photographic emulsion work indicates that  $\kappa$  mesons are produced at least as frequently as the hyperons, so that from the curves in Fig. 8 an estimate of the lifetime of the  $\kappa$  meson of the order of about  $3 \times 10^{-9}$  sec can be obtained. As seen from the shape of the lower chamber curve, this conclusion is essentially independent of the lifetime and mass of the charged hyperon. Any predominance of  $\kappa$  mesons over hyperons at production will cause a corresponding increase in the estimate of the lifetime of the  $\kappa$  meson.

In the interpretation of Table II which gives the charge distributions observed in the two chambers, it ought to be emphasized that the asymmetries indicated by the table are statistically significant only if an explanation in terms of a single type of particle is attempted. If, however, there are several types of charged  $V$  particles, separated automatically according to lifetime by the geometry of the two chambers, then a further interpretation of the observed charge distributions as indicating a predominance of one sign of charge or the other at the point of production for each of these types of particles must be undertaken with caution.

#### APPENDIX

During the course of the experiment 65 events were observed which were consistent with the decay of a  $\pi$  meson into a  $\mu$  meson. Fourteen of these cases were completely measurable and yielded an average  $Q$  value of 34 Mev, in excellent agreement with the known value. An histogram of the transverse momenta of all 65 cases was also plotted and showed good agreement with the expected distribution for  $\pi$ - $\mu$  decay. A careful study of the biases introduced by the difficulty of observing small angle deflections of a track was made, and was estimated to have had but a small effect on the 65 cases used in this histogram. The fact that very few cases were observed in the transverse momentum range,  $p_T < 10$  Mev/ $c$  and that all of these could have been  $\pi$ - $\mu$  decays, indicates that very few, if any, scattering events unaccompanied by recoil blobs were included in the histogram. Because this region of transverse momentum would be expected to contain more scattering events unaccompanied by recoil blobs than any higher momentum range, it can be concluded from this study that very few scattering events went undetected and that the transverse momentum criterion applied to the charged  $V$  events is conservative. Table VII gives the number of positively and negatively charged  $\pi$ - $\mu$  decays in the upper and lower chambers in the same way that Table II gives this information for the charged  $V$  events. The statistical probability that this or any greater asymmetry is due to a random fluctuation is 0.33.

The authors are indebted to Mr. J. D. Sorrels for performing some of the measurements on the  $\pi$ - $\mu$  decays.

TABLE VII. Classification of  $\pi$ - $\mu$  decays according to place of origin and sign of charge.

Origin \ Sign	Positive	Negative	Total
Above place	14	24	38
In plate	16	17	33
Total	30	41	

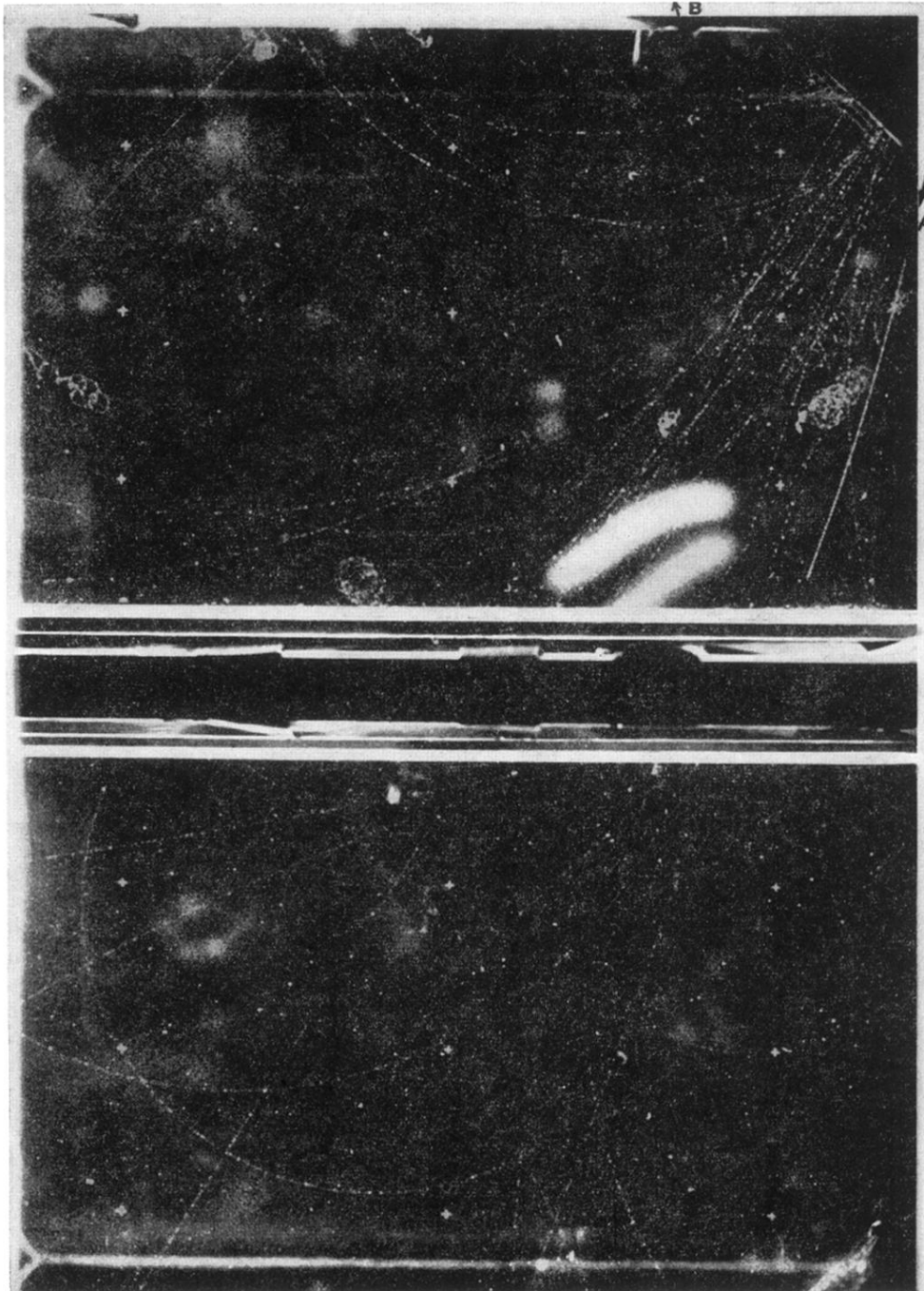


FIG. 3. Event No. 78113, which is listed in Table IV. The heavily ionizing charged  $V$  particle originates in the shower in the upper right-hand corner ( $A$ ) and decays just above the lead plate separating the chambers. The secondary particle is ejected upward and to the left ( $B$ ).